Experimentally Derived Weight Distribution Function for Probabilistic Damage Imaging Using Guided Waves

SOUVIK JANA and SANTOSH KAPURIA

ABSTRACT

The reconstruction algorithm for probabilistic inspection of defects (RAPID) is widely employed to localize damage in thin-walled structures using guided waves. This method constructs probabilistic damage maps using damage indices (DIs) of the sensing paths in a sensor network and associated weight distribution functions (WDFs). Accurate weight distribution function (WDF) estimation is crucial for determining the probability of damage at a given point. Several WDFs have been proposed, including linear, Gaussian, and inverse power law functions, but they rely on assumptions without any experimental validation. We experimentally determine the WDF as the ratio of the DIs of a sensing path due to damage at a given point to its value when the damage is situated on the sensing path orthogonal to that point. Results reveal that the experimentally obtained variation of the damage index ratio does not conform to any of the existing WDF models for either baseline-based or baseline-free methods. Based on experimental data, we propose a simple exponential decay-type WDF, which is shown to be applicable for baseline-based methods and baseline-free refined time reversal method (RTRM) (developed by the second authors group). Thus, the newly proposed WDF provides an accurate estimate of damage probability for both baseline-based methods and the baseline-free RTRM.

INTRODUCTION

Structural Health Monitoring (SHM) relies critically on accurate damage localization to ensure timely maintenance and structural integrity across engineering applications. Among various SHM techniques, guided wave-based methods have gained substantial attention due to their capability to inspect large areas with minimal sensor instrumentation and high sensitivity to small-scale defects [1]. Among the various damage localization algorithm, the reconstruction algorithm for probabilistic inspection of defects (RAPID) is widely employed to localize damage in thin-walled structures using guided waves [2]. This method constructs probabilistic damage maps using damage indices (DIs) of the sensing paths in a sensor network and associated weight distribution functions (WDFs).

A critical factor influencing the performance of RAPID is the selection of the weight distribution function (WDF), which governs how the contribution from each sensing path is spatially distributed across the monitored region. Early implementations typically assumed a linear WDF that decreases proportionally with the normalized relative distance from the sensing path [3–5], or employed Gaussian WDF [6–8]. These functions, however, were primarily formulated based on assumptions without any experimental validation and were originally designed for baseline-based methods that rely on comparing signals with those from an undamaged reference state. Subsequent studies attempted to improve localization accuracy by adjusting the scaling factor (β) [9], or proposing a new WDF based on assumptions which follows an inverse power law function that account for the relationship between the damage index (DI) and the relative normalized distance

Souvik Jana, Graduate Student, Email: amz228087@iitd.ac.in. Department of Applied Mechanics, Indian Institute of Technology Delhi, New Delhi 110016, India
Santosh Kapuria, Professor, Email: kapuria@am.iitd.ac.in; Tel. +91-11-26591218. Department of Ap- plied Mechanics, Indian Institute of Technology Delhi, New Delhi 110016, India

of damage from the sensing path with the weight values [10]. Recent developments, such as the non-linear exponential WDF proposed by Luo et al. [11], aimed to address non-uniformities in sensor networks and to enhance localization accuracy. Despite these advancements, the fundamental behavior of DI variation with respect to damage location has not been experimentally studied across different guided wave-based damage detection methods.

A major challenge associated with the baseline-based techniques is the potential alteration of the sensory response due to variations in environmental and operational conditions, even in the absence of damage. Therefore, the dependence on the baseline signals may unnecessarily lead to false-positive situations [12]. Because of this, there has been an enormous quest among researchers for developing baseline signal-free SHM techniques. Among the various baseline-free methods, the time-reversal method (TRM) has emerged as a particularly popular and effective technique [13]. In this method, the DI is computed using the correlation between the main mode of reconstructed signal after the time-reversal process (TRP) and the original input signal. However, reported inadequate sensitivity of the TRM to the presence of damage prompted the second author‘s group [14] to develop a refined time reversal method (RTRM), wherein the structure is excited at best reconstruction frequency (BRF) [15] to minimize amplitude dispersion and the DI is computed using an extended signal length around the main mode up to the side bands. So far, the WDFs originally developed for baseline-based methods have been applied to the baseline-free methods without verifying their suitability.

In this study, we experimentally determine the WDF as the ratio of the DI of a sensing path due to damage at a given point to its value when the damage is situated on the sensing path orthogonal to that point. The experiments are conducted on an aluminium plate with piezoelectric wafer active senors (PWAS) bonded its top surface for actuating and sensing ultrasonic guided waves. Based on the results, we propose a simple exponential decay-type WDF for baseline-based guided wave methods. Next, we examine the applicability of the proposed WDF for the baseline-free methods, TRM and RTRM, by conducting further experiments.

DAMAGE LOCALIZATION ALGORITHM

The RAPID is a widely adopted method for localizing damage in thin-walled structures using guided waves. In this approach, a probabilistic image indicating the likelihood of damage at a given point (x, y) is generated by summing the weighted signal features across elliptical patterns formed by various pitch-catch transducer pairs. Considering a sensor network comprising n sensing paths, the probability of damage at a location (x, y) is expressed as,

$$P(x,y) = \sum_{j=1}^{N} W_j[r_j(x,y)]\, DI_j \tag{1}$$

where $W_j\left[r_j(x,y)\right]$ represents the probabilistic WDF associated with the j^{th} sensing path at point (x, y), and $r_j(x, y)$ denotes the normalized relative distance of (x, y) from the corresponding sensing path, defined as,

$$r_j(x,y) = \frac{d_{j,ap} + d_{j,bp}}{d_{j,ab}} - 1 \tag{2}$$

where $d_{j,ab}$ is the distance between the actuator a and sensor b for the j^{th} path, and $d_{j,ap}$ and $d_{j,bp}$ are the distances from the point (x, y) to the actuator and sensor, respectively (Fig. 1). The term DI_j denotes the damage index for the j^{th} sensing path. In this study, the damage index is computed based on the L_2-norm error, defined as,

$$DI_j = \left(\sqrt{\frac{\int_{t_i}^{t_f} [V_j(t) - I_j(t)]^2 \, dt}{\int_{t_i}^{t_f} I_j^2(t) \, dt}} \right). \tag{3}$$

For baseline-based methods, $I_j(t)$ refers to the forward response obtained from the

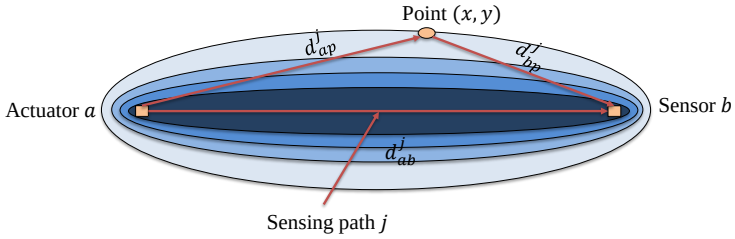

Figure 1. Illustration of the relative distance for a single actuator-sensor pair.

j^{th} sensing path in the undamaged state, and $V_j(t)$ corresponds to the response after damage has occurred. For baseline-free methods, $I_j(t)$ represents the normalized input signal, and $V_j(t)$ is the reconstructed signal obtained through the time-reversal process. The time limits t_i and t_f denote the start and end instants for the signal analysis: for baseline-based methods, these correspond to the forward response; for the conventional TRM, they refer to the main mode of the reconstructed signal [16], and for the RTRM, they correspond to the extended mode of the reconstructed signal [14].

EXISTING WEIGHT DISTRIBUTION FUNCTIONS

The linear WDF, commonly used in damage localization, is expressed as [5]

$$W_j\left[r_j(x,y)\right] = \begin{cases} 1 - \dfrac{r_j(x,y)}{\beta}, & \text{if } r_j(x,y) < \beta \\ 0, & \text{if } r_j(x,y) \geq \beta \end{cases} \tag{4}$$

where β is a scaling parameter that controls the extent of the influence area associated with each sensing path.

Another widely adopted model is the Gaussian WDF, defined as [9]

$$W_j\left[r_j(x,y)\right] = \begin{cases} \exp\left[-\left(\dfrac{r_j(x,y)}{\beta} \right)^2 \right], & \text{if } r_j(x,y) < \beta \\ 0, & \text{if } r_j(x,y) \geq \beta. \end{cases} \tag{5}$$

These WDFs have been extensively employed in both baseline-based and baseline-free guided wave damage localization methods without thorough experimental validation of

their applicability. In the following section, we present a newly obtained weight distribution function based on experimental observations.

PROPOSED EXPONENTIAL WEIGHT DISTRIBUTION FUNCTION

To experimentally determine the WDF, we performed a series of experiments with varying normalized relative distances of damage from the sensing paths. For each damage position, we assessed the impact of the damage on the corresponding sensing path by calculating the DI. The WDF is defined as the ratio of the DI of a sensing path due to damage at a given location to the DI value when the damage is directly aligned with the sensing path. Thus, a maximum weight of unity is assigned when the damage is situated directly on the sensing path, and the weight decreases as the relative distance increases. Therefore, the weight value (W_j) for a damage position at (x, y) for the j^{th} sensing path is computed as

$$W_j = \frac{DI_j}{(DI_j)_0}, \tag{6}$$

where $(DI_j)_0$ is the damage index for j^{th} sensing path when the damage is situated directly on the sensing path.

We calculated the weight value W_j for baseline-based and baseline-free methods and find that for both methods it follows a simple exponential decaying curve with the relative normalized distance, which can be expressed as

$$W_j\left[r_j(x,y)\right] = \exp\left(-\sqrt{(\frac{r_j(x,y)}{\beta}}\right) \tag{7}$$

EXPERIMENTAL SETUP

Experiments are performed on an aluminum (Al) plate with dimensions 2438 mm $\times$ 1220 mm $\times$ 3 mm (Fig. 2). Three square-shaped PWAS (SP-5H type, Sparkler Ceramics Pvt. Ltd., India), each measuring 10 mm $\times$ 10 mm with a thickness of 0.25 mm, are bonded to the top surface of the plate using a two-component Araldite-epoxy adhesive. The thickness of the adhesive layer is measured using a Micro-Epsilon ILD-1400-10 laser displacement sensor with a resolution of 1 μm, following the methodology outlined in [17]. The average measured thickness of the adhesive layer is 52 ± 1 μm. The damage is placed at an arbitrary location between the actuator-sensor pair to observe its influence on the corresponding sensing path (Fig. 3).

Signal generation and data acquisition are performed using the QDAM772E18 system (Quazar Technologies Pvt. Ltd., India), which integrates a high-frequency, high-voltage signal generator with data acquisition capabilities. The system includes a function generator capable of delivering signals up to 80 V peak-to-peak at frequencies up to 1 MHz and a 14-bit DAQ unit operating at sampling rates up to 80 mega samples per second (MSPS). A charge amplifier with adjustable gain is also incorporated. Signal processing and data acquisition are visualized using the iQ software developed by the same company. Data are acquired at a sampling rate of 72 MSPS, and each signal is averaged over 20 repetitions to improve the signal-to-noise ratio.

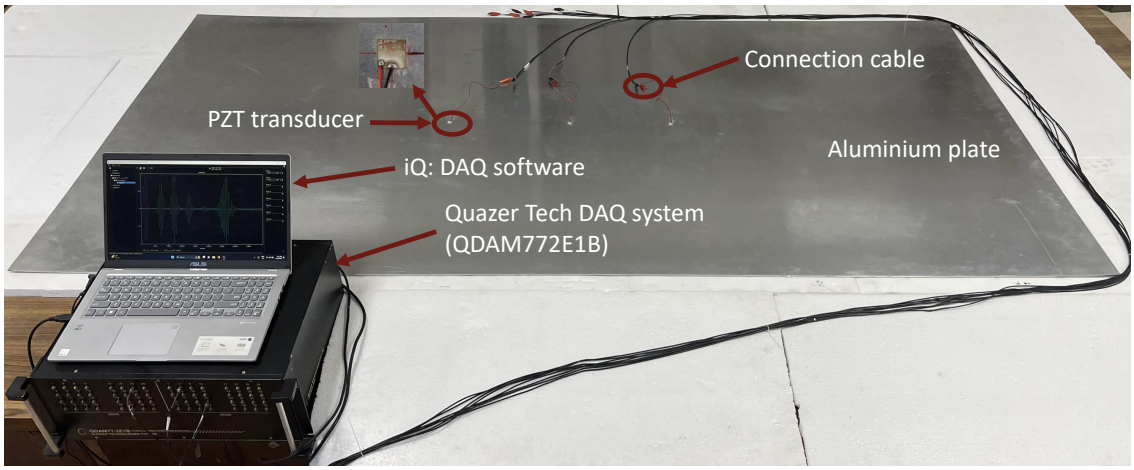

Figure 2. Experimental setup for Lamb wave generation and sensing with PZT transducers in an aluminium plate.

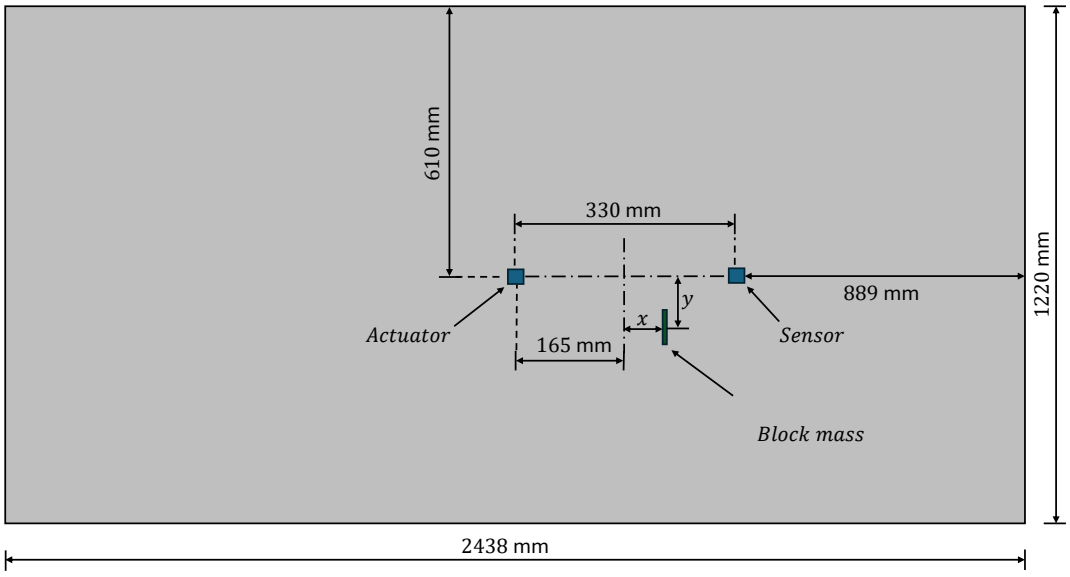

Figure 3. Schematic illustration of damage located at an arbitrary position between two transducers.

RESULTS AND DISCUSSION

The DI ratio and the corresponding weight value is experimentally determined for the baseline-based method, the conventional TRM, and the baseline-free RTRM using Eqs. (3) and (6).

BASELINE-BASED METHOD

Figure 1 shows the variation of weight values, for different damage positions corresponding to varying normalized relative distances at excitation frequencies of 100 kHz,

200 kHz, 300 kHz, and 400 kHz in baseline-based methods. For comparison, the existing WDF models, namely the linear and Gaussian models, are also plotted along with the proposed exponential decay-type WDF, using a common scaling parameter $\beta = 0.02$. The results clearly show that the experimentally obtained weight values do not conform to the existing WDF models across all tested frequencies. In contrast, the experimental data closely fit the proposed exponential decay-type WDF, demonstrating its superior suitability for representing the spatial variation of the weight value in baseline-based guided wave methods.

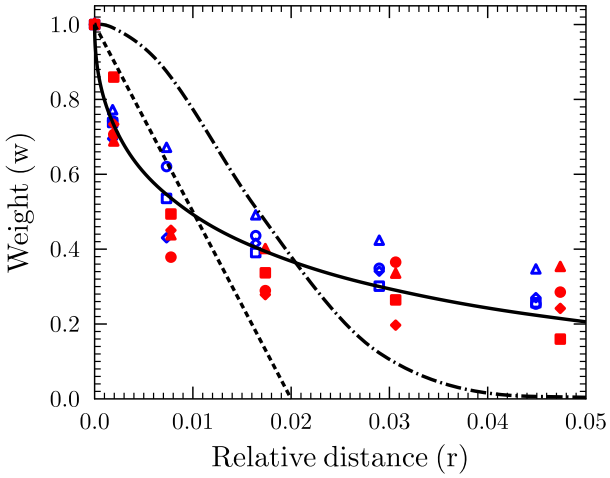

Figure 4. Variation of experimentally obtained weights (w) with normalized relative distance for the baseline-based method. $\square$, $\circ$, $\triangle$, and $\diamond$ shape represent 100 kHz, 200 kHz, 300 kHz, and 400 kHz respectively. Blue Hollow marker and red solid marker represents the damage present at $x = 0$ mm (mid line between two transducers), and $x = 40$ mm (away from mid line). Dashed, dash-dotted, solid line represent linear, Gaussian, and proposed exponential decay-type WDF curve.

BASELINE-FREE METHODS

Figure 2 presents the variation of weight values obtained for conventional TRM, where the DI is determined by correlating the main mode of the reconstructed signal with the original input signal. Unlike the baseline-based methods, the experimentally obtained weight values in conventional TRM do not exhibit a monotonic decrease with normalized relative distance but instead show oscillatory behavior. This non-monotonic trend is attributed to amplitude dispersion in the main mode of the reconstructed signal, which results in significant non-zero DI values even in the absence of damage. Thus, none of the WDFs work for the TRM. To address this issue, the RTRM is examined, wherein the structure is excited at the BRF to minimize amplitude dispersion. In this study, the BRF is identified as 150 kHz following the procedure outlined in [15]. In Figure 3, we have plotted the different weight values obtained for different normalized

relative distances at BRF. It is observed that the experimentally measured weight values closely follow the proposed exponential decay-type WDF, confirming its validity for baseline-free RTRM as well. Overall, these findings demonstrate that the proposed WDF provides an accurate and experimentally validated model for estimating damage probability for both baseline-based guided wave methods and the baseline-free RTRM.

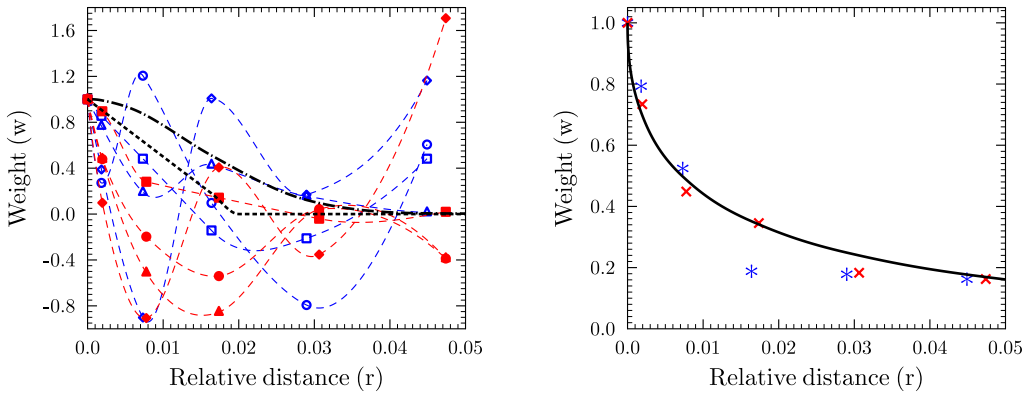

(a) conventional TRM (b) RTRM

Figure 5. Variation of experimentally obtained weights (w) with normalized relative distance for the baseline-free methods, (a) $\square$, $\circ$, $\triangle$, and $\diamond$ shape represent 100 kHz, 200 kHz, 300 kHz, and 400 kHz respectively. Blue Hollow marker and red solid marker represents the damage present at $x = 0$ mm (mid line between two transducers), and $x = 40$ mm (away from mid line). Dashed and dash-dotted line represent linear and Gaussian WDF curve respectively, (b) $*$, and $\times$ marker represents the damage present at $x = 0$ mm (mid line between two transducers), and $x = 40$ mm (away from mid line) at BRF (150 kHz). Solid line represents proposed exponential decay-type WDF curve.

CONCLUSION

This study systematically determines through experiments the WDF for probabilistic damage imaging using guided waves. A series of experiments is conducted to evaluate the variation of the weight value (DI ratio) with the normalized relative distance between the damage and sensing paths. It is observed that the existing WDF models, such as linear and Gaussian functions, do not accurately capture the experimentally obtained variation of DI ratio for both baseline-based methods and baseline-free conventional TRM. A new exponential decay-type WDF is proposed based on experimental observations, which assigns the maximum weight when the damage lies directly on the sensing path and exhibits a gradual decrease as the relative distance increases. The proposed WDF accurately models the experimentally obtained DI variations for both baseline-based method and the baseline-free RTRM.

This advancement will significantly enhance the precision of guided wave-based damage localization, making structural health monitoring more reliable and effective.

REFERENCES

1. Lee, B. and W. J. Staszewski. 2003. "Modelling of Lamb waves for damage detection in metallic structures: Part II. Wave interactions with damage," *Smart materials and structures*, 12(5):815.
2. Hay, T., R. Royer, H. Gao, X. Zhao, and J. Rose. 2006. "A comparison of embedded sensor Lamb wave ultrasonic tomography approaches for material loss detection," *Smart Materials and Structures*, 15(4):946.
3. Zhao, X., H. Gao, G. Zhang, B. Ayhan, F. Yan, C. Kwan, and J. L. Rose. 2007. "Active health monitoring of an aircraft wing with embedded piezoelectric sensor/actuator network: I. Defect detection, localization and growth monitoring," *Smart Materials and Structures*, 16(4):1208.
4. Wang, D., L. Ye, Z. Su, Y. Lu, F. Li, and G. Meng. 2010. "Probabilistic damage identification based on correlation analysis using guided wave signals in aluminum plates," *Structural Health Monitoring*, 9(2):133–144.
5. Kannusamy, M., S. Kapuria, and S. Sasmal. 2022. "An efficient Lamb wave-based virtual refined time-reversal method for damage localization in plates using broadband measurements," *Ultrasonics*, 124:106767.
6. Su, Z., L. Cheng, X. Wang, L. Yu, and C. Zhou. 2009. "Predicting delamination of composite laminates using an imaging approach," *Smart Materials and Structures*, 18(7):074002.
7. Migot, A., Y. Bhuiyan, and V. Giurgiutiu. 2019. "Numerical and experimental investigation of damage severity estimation using Lamb wave–based imaging methods," *Journal of Intelligent Material Systems and Structures*, 30(4):618–635.
8. Guo, J., X. Zeng, Q. Liu, and X. Qing. 2022. "Lamb wave-based damage localization and quantification in composites using probabilistic imaging algorithm and statistical method," *Sensors*, 22(13):4810.
9. Nasiri, M., A. Abedian, and J. Amraei. 2023. "Improving Probability-Based Diagnostic Imaging Algorithm by Modeling Weight Distribution Coefficient for Instantaneous Baseline Damage Identification," *Journal of Aerospace Engineering*, 36(2):04022126.
10. Liu, G., B. Wang, L. Wang, Y. Yang, and X. Wang. 2022. "Probability-based diagnostic imaging with corrected weight distribution for damage detection of stiffened composite panel," *Structural Health Monitoring*, 21(4):1432–1446.
11. Luo, K., L. Chen, Y. Chen, L. Ye, and S. Yu. 2025. "An ultrasonic Lamb wave-based nonlinear exponential RAPID method for delamination detection in composites," *Composite Structures*, 352:118701.
12. Sohn, H. 2007. "Effects of environmental and operational variability on structural health monitoring," *Special Issue of Philosophical Transactions of Royal Society on Structural Health Monitoring*, 365:539–560.
13. Ing, R. K. and M. Fink. 1998. "Time-reversed Lamb wave," *IEEE Transactions,Ultrasonic, Ferroelectrics and Frequency Control*, 45:1032–1043.
14. Agrahari, J. K. and S. Kapuria. 2016. "A refined Lamb wave time-reversal method with enhanced sensitivity for damage detection in isotropic plates," *Journal of Intelligent Material Systems and Structures*, 27(10):1283–1305.
15. Kapuria, S. 2023. "Best Reconstruction Frequency of Lamb Waves Via Broadband Measurement," *Structural Health Monitoring 2023*.
16. Park, H. W., H. Sohn, K. H. Law, and C. R. Farrar. 2007. "Time reversal active sensing for health monitoring of a composite plate," *Journal of Sound and Vibration*, 302:50–66.
17. Agrahari, J. and S. Kapuria. 2016. "Effects of adhesive, host plate, transducer and excitation parameters on time reversibility of ultrasonic Lamb waves," *Ultrasonics*, 70:147–157.